Observing Correlated Production of Defects and Antidefects in Liquid Crystals

Sanatan Digal, Rajarshi Ray, and Ajit M. Srivastava
Institute of Physics, Sachivalaya Marg, Bhubaneswar 751005, India
(Received 29 July 1999)

We present observations of strength-one defects and antidefects formed in isotropic-nematic phase transition of a thin layer of nematic liquid crystals, using optical microscopy. We measure the widths of the distributions of net winding number in small regions, and determine the exponent characterizing the correlation between defects and antidefects to be 0.26 ± 0.11, in very good agreement with the value $1/4$ predicted by the Kibble mechanism for defect production. We also describe a novel technique to determine the director distribution in observations of defect networks.

PACS numbers: 61.30.Jf, 64.70.Md

The study of topological defects is a highly interdisciplinary area in physics. This has led to a valuable interplay of ideas from different branches of physics. For example, the first theory of formation of topological defects, formulated by Kibble [1] in the context of the early Universe, found experimental verification of some of its aspects in certain condensed matter systems [2–5], namely, the prediction of average defect density; see Refs. [3,4]. In this paper, we present an experimental determination of correlation between defects and antidefects. This leads to direct verification of a prediction of the Kibble mechanism, which is qualitatively different from the other prediction of defect density. Our results are important as they present first (to our knowledge) experimental measurement of defect-antidefect correlations.

In the Kibble mechanism, defects form due to a domain structure arising in a phase transition. For example, in a spontaneous symmetry breaking transition of a U(1) symmetry, with the order parameter being an angle θ lying between 0 and 2π, the order parameter space is a circle S^1. The domains are characterized by roughly uniform θ which varies randomly from one domain to another (and varies with least gradient in between adjacent domains). Here one gets string defects with nonzero winding of θ around the string. By considering the probability of getting a winding around a junction of three domains, it is easy to show [3] that the probability of vortex formation per domain, in two space dimensions, is equal to $1/4$. Consider now a vortex formed at the junction of three domains. Then the probability of formation of an antivortex in the neighboring region increases since part of the (anti)winding of θ is already present, and one needs only to have right θ value, say, in a fourth, adjacent domain. This conclusion, about certain correlation in the formation of a defect and an antidefect, is valid for other types of defects as well [6]. To see this effect [7] let us consider a two-dimensional region Ω whose area is A and whose perimeter L goes through L/ξ number of elementary domains (where ξ is the domain size). As θ varies randomly from one domain to another, one is essentially dealing with a random walk problem with the average step size for θ being $\pi/2$ (the largest step is π and the smallest is zero). Thus, the net winding number of θ around L will be distributed about zero with a typical width given by $\sigma = \frac{1}{4}\sqrt{\frac{L}{\xi}}$, implying that $\sigma \propto A^{1/4}$. Assuming roughly uniform defect density, we get $\sigma \propto N^{1/4}$ (where N is the total number of defects in the region Ω), which reflects the correlation in the production of defects and antidefects. In the absence of any correlations, the net defect number will not be as suppressed, and will follow Poisson distribution with $\sigma \sim \sqrt{N}$. In general one may write the following scaling relation for σ:

$$\sigma = CN^{\nu}. \tag{1}$$

The exponent ν will be $1/2$ for the uncorrelated case. As we show below, our experimental results give $\nu = 0.26 \pm 0.11$ which is in very good agreement with the predicted value of $1/4$ from the Kibble mechanism, and reflects the correlated nature of defects and antidefects. To get C as predicted by the Kibble mechanism, we take the elementary domains to be equilateral triangles. Let us also assume, for simplicity, that the two-dimensional region Ω under observation is a square with area $A = (L/4)^2$. With the probability of defect formation per domain being $1/4$, we get $N = L^2/(16\sqrt{3}\,\xi^2)$. With $\sigma = \frac{1}{4}\sqrt{\frac{L}{\xi}}$, one can rewrite σ as $\sigma = (3^{1/8}/2)N^{1/4}$ giving $C = 3^{1/8}/2 = 0.57$. If the elementary domains are squares, then we get $C = 0.71$. (One may have domains of various shapes and sizes in a local region. It is not known what should be the correct distribution of domains for the Kibble mechanism. Thus, as usual, we simply take all domains to be roughly similar.)

For uniaxial nematic liquid crystals (NLC) the orientation of the order parameter in the nematic phase is given by a unit vector (with identical opposite directions) called the director. The order parameter space is $RP^2 (\equiv S^2/Z_2)$, which allows for string defects with strength $1/2$ windings. Because of birefringence of NLC, when the liquid crystal sample is placed between crossed polarizers, then regions where the director is either parallel or perpendicular to the electric field $\vec{E}$, the polarization is maintained resulting in a dark brush. At other regions, the polarization changes through the sample, resulting in a bright

 0031-9007/99/83(24)/5030(4)$15.00

region. This implies that for a defect of strength s, one will observe $4s$ dark brushes [8]. If the cross-polarizer setup is rotated, then brushes will rotate in the same (opposite) direction for positive (negative) windings. Equivalently, if the sample is rotated between fixed crossed polarizers, then brushes do not rotate for $+1$ winding while they rotate in the same direction (with twice the angle of rotation of the sample) for -1 winding. We use this method to determine the windings.

We now describe our experiment. We observed isotropic-nematic (IN) transition in a tiny droplet (size $\sim 2-3$ mm) of NLC 4′-Pentyl-4-biphenyl-carbonitrile (98% pure, purchased from Aldrich Chem.). The sample was placed on a clean, untreated glass slide and was heated using an ordinary lamp. The IN transition temperature is about 35.3 °C. Our setup allowed the possibility of slow heating, and cooling, by changing the distance of the lamp from the sample. (This part was the same as in Ref. [3].) We observed the defect production very close to the transition temperature (in some cases we had some isotropic bubbles coexisting with the nematic layer containing defects). For the observations, we used a Leica, DMRM microscope with 20× objective, a CCD camera, and a cross-polarizer setup, at the Institute of Physics, Bhubaneswar. Phase transition process was recorded on a standard videocassette recorder. The images were photographed directly from a television monitor by replaying the cassette.

The IN transition is of first order. When the transition proceeds via nucleation of bubbles, we observe long horizontal strings which are not suitable for our analysis. We selected those events where the transition seems to occur uniformly in a thin layer near the top of the droplet (possibly due to faster cooling from contact with air). The depth of field of our microscope was about 20 μm. All the defects in the field of view were well focused, suggesting that they formed in a thin layer, especially since typical interdefect separation was about $10-40$ μm. (For us, the only thing relevant is that the layer be effectively two dimensional over distances of order of typical interdefect separation.) Also, the transition happened over the entire observation region roughly uniformly, suggesting that a process like spinodal decomposition [9] may have been responsible for the transition. This resulted in a distribution of strength-one defects as shown in the photographs in Fig. 1. Points from which four dark brushes emanate correspond to defects of strength ± 1. Because of resolution limitation the crossings here do not appear as pointlike. It is practically impossible to use the technique of rotation of brushes to identify every winding in situations such as shown in Fig. 1 due to very small interdefect separation (resulting from high defect density), as well as due to extremely rapid evolution of the defect distribution.

We have developed a particular technique for determining individual windings of defects in situations like Fig. 1 where one needs only to determine the winding of one of the defects by rotation in a cross polarizer setup. Windings of the rest of the defects can then be determined using topological arguments, as we explain below. Figure 2b shows the situation where the sample is rotated in a clockwise manner, compared to Fig. 2a (as shown by the defect patterns). We first determine the winding of one of the defects, marked by a "$*$" in Fig. 2a. By noting the rotation of brushes in Fig. 2b, we determine that it is a defect (v, marked by arrow) with $+1$ winding (as the brushes do not rotate for this defect; note that here we are rotating the sample). Now, one of the brushes emanating from this defect is assumed to correspond to the director being parallel to $\vec{E}$ with θ assumed to be zero. Winding $= +1$ then implies that the next brush, going clockwise around the defect, should correspond to $\theta = 3\pi/2$ with the director perpendicular to $\vec{E}$. The next two brushes will then correspond to $\theta = \pi$ and $\pi/2$, respectively. We now denote the quadrant on the circle S^1, between $\theta = 0$ to

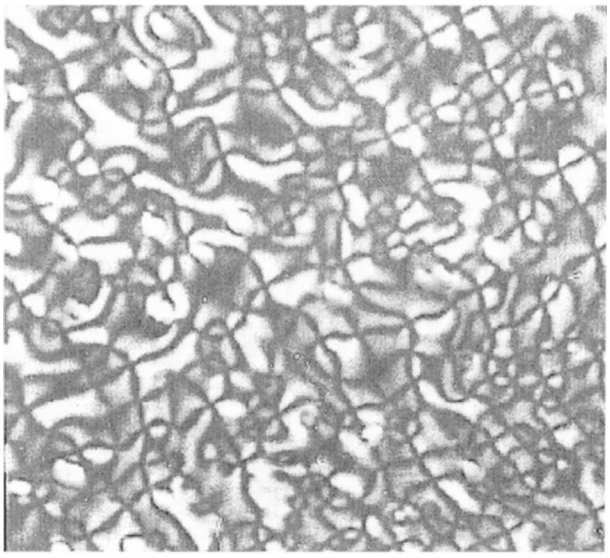

FIG. 1. Picture of defect distribution observed using crossed polarizers in IN transition. Size of the image is about 0.27 mm × 0.24 mm.

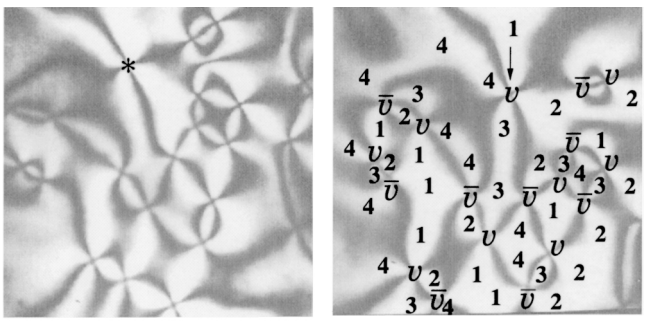

FIG. 2. Verification of the procedure for identifying the windings of defects. Size of each image is about 0.3 mm × 0.3 mm.

$3\pi/2$ by number 1, the quadrant, between $\theta = 3\pi/2$ to π by number 2, and similarly, the other two quadrants (going clockwise) by numbers 3 and 4. This allows us to write numbers 1 to 4 in between the brushes.

Using continuity of the order parameter outside the location of defects, one can easily see that θ in between any two brushes remains in the same quadrant irrespective of the size and the shape of that region, as a change of quadrant should happen only across a dark brush. Around any defect, if we know the quadrant numbering of any two adjacent regions between the brushes, then the quadrant numbers for the remaining two regions are assigned assuming the same sense for the winding as determined by the first two quadrant numbers. (This is when the crossing corresponds to a defect. Occasionally there are situations where one is not able to resolve whether two brushes are just very close or there is a crossing there. In such cases, if a wrong choice is made, then one finds a conflict in quadrant assignment when approaching from different directions.) Using these simple rules, we complete the quadrant assignment in the picture in Fig. 2b, and determine windings of all defects. As defects are far separated here, one can also determine their windings by noticing rotation of the brushes directly. The results are in complete agreement with the windings determined using our technique of quadrant assignment. This is not surprising as the arguments given above for the technique use only continuity properties of the director, and hence are topological in nature, independent of the details of the defect network.

Note that whenever two defects are joined by two (or more) brushes, they represent defect-antidefect pairs. (It is easy to see that in between two defects of the same windings there must be a region belonging to the same quadrant extending to infinity, unless truncated by other defects [10].) Figures 1 and 2 show that defect-antidefect pairs are most abundant, supporting the correlation in defect-antidefect production. Pictures like those in Fig. 2 are present in the literature [8] (though we have not seen pictures as in Fig. 1 with very dense network of defects). However, in some of those cases, one also observes few strength-$1/2$ defects, i.e., points from which only two brushes emanate. We do not get any of these. If we had missed any such points due to resolution of the picture, it would have led to conflict in the director assignment on the two sides of the brush following our technique, as we have verified from the pictures in the literature. A possible explanation for the absence of $1/2$ defects could have been that these are point monopole defects. However, it is known that monopole production in this manner is highly suppressed [11]. Further, similar pictures in the literature [8] show some strength-$1/2$ defects as well, which is not possible if these are monopoles. We propose the following explanation for this. The anchoring of the director at the IN interface [12] forces the director to lie on a cone, with the half angle equal to about 64°. This forces the order parameter space there to become effectively a circle S^1, instead of being RP^2, with the order parameter being an angle between 0 and 2π. Only defects allowed now are with integer windings. Of course, depending on the anchoring energy, strength–$1/2$ defects could still form, with a certain region having higher energy. Further, the space here is effectively two dimensional since integer windings can be trivialized as one moves away from the IN interface, towards the nematic-air interface with the normal boundary condition. (In this sense, these defects may be like partial monopole configurations.) Therefore the prediction for σ from the Kibble mechanism for the U(1) case, as described above, is valid for this case, with the picture that a domain structure near the IN interface is responsible for the formation of integer windings.

After identifying the windings of all defects (wherever possible) in a picture, we first determine the average defect density, and then divide the picture in terms of square shaped regions (Ω) containing N defects on average. We do the analysis for three different values of N, $N = 10$, 20, and 30. Regions are marked without noticing the presence of defects to avoid any bias. In order to increase statistics, we also included some square regions with partial overlap (making sure that the boundaries of the two regions, though intersecting, should not overlap). It should be clear that net windings along the perimeters of such squares also represent independent statistics. For each square region, net defect number Δn (i.e., number of defects minus number of antidefects) was found and by analyzing a large number of pictures, the frequency $f(\Delta n)$ for each value of Δn was determined. Figure 3 shows the plots of $f(\Delta n)$ vs Δn. Solid, dotted, and dashed curves show Gaussian fits to the experimental points corresponding to $N = 10$, 20, and 30, respectively. The number of regions analyzed for these cases was 91, 54, and 34 in that order. Table I summarizes our results for the Gaussian fits for the three sets of data, where we give the best fit values of the parameters of the Gaussian, along with the standard errors in the determination of these parameters from the fit.

For square shaped elementary domains, predicted values of σ are 1.26, 1.50, and 1.66, for $N = 10$, 20, and 30, respectively, which are in reasonable agreement with the measured values given in Table I. (For triangular domains, predicted values are lower, with $\sigma = 1.01$, 1.21, and 1.33 for the three values of N.) If defects and antidefects were uncorrelated then we expect, by randomly distributing defects and antidefects in the region, that $\sigma = 3.15$, 4.47, and 5.50, for $N = 10$, 20, and 30, respectively. These values are markedly different from the values experimentally observed. Note that if defect-antidefect pairs were thermally

TABLE I. Results of fitting data to $f(\Delta n) = ae^{-(\Delta n - \overline{\Delta n})^2/2\sigma^2}$.

N	a	$\overline{\Delta n}$	σ
10	26.37 ± 1.15	0.06 ± 0.07	1.41 ± 0.07
20	13.54 ± 1.12	−0.17 ± 0.16	1.64 ± 0.16
30	7.21 ± 0.78	0.44 ± 0.24	1.94 ± 0.25

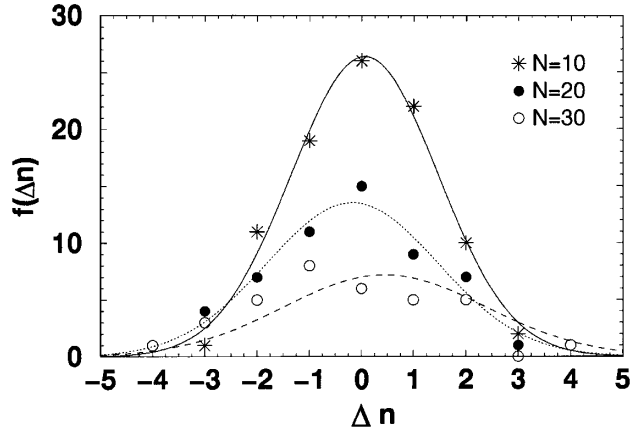

FIG. 3. Plots of the frequency $f(\Delta n)$ vs Δn.

produced, then any resulting correlation could be observed only for typical interdefect separations of order of the core size of the defect ($\simeq$ few hundred angstroms). The interdefect separations we observe (at the time of formation itself) are of the order of $10-40$ μm. We mention here that sometimes we observe defects after the network has undergone some evolution. However, it does not affect correlations between defects and antidefects produced via the kibble mechanism (as long as kinetic energies of defects are not too large, which certainly is the case here). Defect-antidefect symmetry implies that the Gaussians should be centered at zero. As we see from Table I, centers of Gaussians $\overline{\Delta n}$ are indeed consistent with zero.

Given the values of σ for different N, we can determine the exponent ν in Eq. (1). The stars in Fig. 4 denote experimental values of $\ln(\sigma)$ vs $\ln(N)$ for the three values of N. The straight line shows the best linear fit to these points. The slope of the line gives the value of the exponent ν. We find

$$\nu = 0.26 \pm 0.11 . \tag{2}$$

This value is in excellent agreement with the theoretical value of $1/4$ predicted by the Kibble mechanism. Though the error is somewhat large, it still rules out zero correlation between defects and antidefects which would give the value of the exponent to be $1/2$. The intercept of the line in Fig. 4 is found to be -0.27 ± 0.27. This gives the value of the prefactor in Eq. (1) to be $C = 0.76 \pm 0.21$. Again, this value is in good agreement with the predicted value of $C = 0.71$ from the Kibble mechanism for the case of square shaped elementary domains, though error is too large in this case for making any definitive statement about the preferred shape of elementary domains.

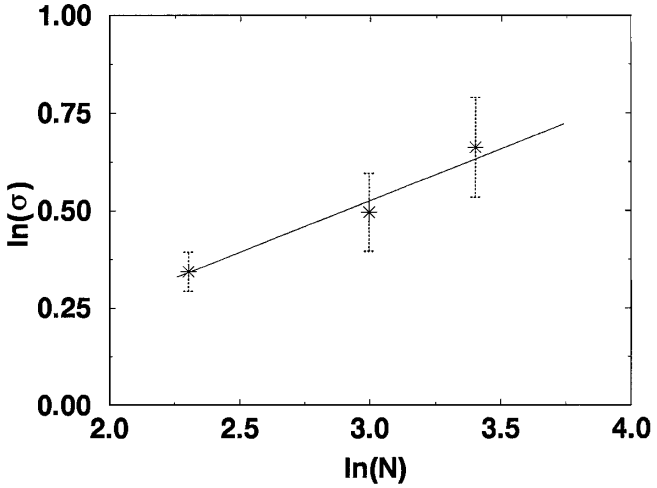

FIG. 4. Determination of the exponent ν.

We conclude by stressing that these observations provide first measurement of defect-antidefect correlations, and lead to experimental verification of this crucial aspect of the Kibble mechanism. Another point is that the prediction of defect density, via Kibble mechanism, crucially requires the knowledge of the domain size [5]. In Ref. [3], the transition proceeded by bubble nucleations, so domains were easily identified. When domains are not that clearly identifiable, as in the present case, then how does one determine the process underlying the defect production? Here, by checking a qualitatively different aspect of the Kibble mechanism, one is able to say that the correlations in defect-antidefect production support the underlying picture being that of the Kibble mechanism. We also emphasize that the technique we have described for determining the windings of defects is an extremely efficient one (and also fun to play with). We believe that this technique can be very useful in determining properties of dense defect networks in liquid crystals.

We are very thankful to Supratim Sengupta for useful discussions and comments. We acknowledge V. S. Ramamurthy for his encouragement and help in setting up liquid crystal experiments at IOP.

[1] T. W. B. Kibble, J. Phys. A **9**, 1387 (1976).
[2] I. Chuang, R. Durrer, N. Turok, and B. Yurke, Science **251**, 1336 (1991).
[3] M. J. Bowick, L. Chandar, E. A. Schiff, and A. M. Srivastava, Science **263**, 943 (1994).
[4] P. C. Hendry, N. S. Lawson, R. A. M. Lee, P. V. E. McClintock, and C. D. H. Williams, J. Low Temp. Phys. **93**, 1059 (1993); G. E. Volovik, Czech. J. Phys. **46**, 3048 (1996), Suppl. S6.
[5] W. H. Zurek, Phys. Rep. **276**, 177 (1996); see also A. Yates and W. H. Zurek, Phys. Rev. Lett. **80**, 5477 (1998).
[6] A. M. Srivastava, Phys. Rev. D **43**, 1047 (1991).
[7] T. Vachaspati and A. Vilenkin, Phys. Rev. D **30**, 2036 (1984).
[8] S. Chandrasekhar and G. S. Ranganath, Adv. Phys. **35**, 507 (1986).
[9] N. Goldenfeld, *Lectures on Phase Transitions and the Renormalization Group* (Addison-Wesley, Reading, MA, 1992).
[10] C. Rosenzweig and A. M. Srivastava, Phys. Rev. D **43**, 4029 (1991).
[11] M. Hindmarsh, Phys. Rev. Lett. **75**, 2502 (1995).
[12] S. Faetti and V. Palleschi, Phys. Rev. A **30**, 3241 (1984).